Adıyaman University
Journal of Engineering Sciences
Adyü J Eng Sci 2026;13:e260123
Adıyaman Üniversitesi
Mühendislik Bilimleri Dergisi
Adyü Müh Bil Derg 2026;13:e260123
https://doi.org/10.54365/adyumbd.1822781

Research Article / Araştırma Makalesi

The investigation of Al–Ti–B Master Alloy as an Independent Material: Impact of Heat Treatment on Corrosion Resistance

Bağımsız Bir Malzeme Olarak Al–Ti–B Alaşımının İncelenmesi: Isıl İşlemin Korozyon Direncine Etkisi

Mahmut Furkan Kalkan [1]*

[1] Gaziantep University, Faculty of Engineering, Department of Mechanical Engineering, Gaziantep, Türkiye.

Abstract

Grain refinement in aluminum alloys is predominantly accomplished by the use of Al–Ti–B master alloys, which comprise TiB_2 and Al_3Ti phases that affect the mechanical and corrosion properties of the material. Notwithstanding their industrial importance, their independent performance under temperature exposure has received scant consideration. This study was conducted to demonstrate the changes in corrosion resistance and hardness of the Al-Ti-B alloy, commonly used as a grain refiner, when heat-treated at different temperatures. In the study, a 10 mm diameter Al-5Ti-B alloy was heat-treated at 200, 300, and 400 °C . The results of these three samples were compared with those of the untreated sample. The results of these samples were compared with those of the untreated sample. It was found that heat treatment at 200 °C and 300 °C increased the corrosion rate, whereas treatment at 400 °C resulted in the lowest corrosion rate.

Keywords: *Al-Ti-B master alloy, heat treatment, corrosion behaviour, hardness, aluminium oxide film*

Öz

Alüminyum alaşımlarında tane inceltme genellikle TiB_2 ve Al_3Ti fazlarını içeren Al–Ti–B ana alaşımlarının kullanımıyla sağlanır. Bu fazlar, malzemenin mekanik ve korozyon özelliklerini önemli ölçüde etkiler. Ancak, bu alaşımların yüksek sıcaklıklara maruz kaldığında bağımsız performansları literatürde yeterince incelenmemiştir. Bu çalışma, tane inceltici olarak yaygın şekilde kullanılan Al–Ti–B alaşımının farklı sıcaklıklarda ısıl işleme tabi tutulduğunda korozyon direnci ve sertlik özelliklerinde meydana gelen değişimleri ortaya koymak amacıyla yapılmıştır. Çalışmada, 10 mm çapında Al–5Ti–B alaşımı 200, 300 ve 400 °C sıcaklıklarda ısıl işleme tabi tutulmuştur. Bu üç numunenin sonuçları, ısıl işlem uygulanmamış kontrol numunesi ile karşılaştırılmıştır. 200 °C ve 300 °C'de ısıl işlem korozyon hızını artırırken, 400 °C'de en düşük korozyon hızı elde edilmiştir

Anahtar Kelimeler: *Al–Ti–B alaşımı, ısıl işlem, korozyon davranışı, sertlik, Alüminyum oksit filmi*

* Corresponding e-mail (Sorumlu yazar e-posta): mfkalkan@gantep.edu.tr
Received (Geliş Tarihi):13.11.2025, **Accepted (Kabul Tarihi):** 08.04.2026

1. Introduction

Ligh alloys such as aluminm and titanium have recently become increasing common in many sectors. These materials offer high specific strength, machinability, conductivity and corrosion resistance, allowing them to compete with traditional high density alloys [1]. Due to their price and wide production capabilities, the use of aluminium alloys is becoming more widespread compared to other light alloys [2,3]. Commonly used alloys are divided into different groups depending on their composition and have a variety of applications: 2xxx series alloys offer high strength with copper additions, 5xxx series magnesium-based alloys stand out with their corrosion resistance, and 6xxx series alloys, with their magnesium and silicon additions, provide a balance between strength and machinability. It is known that various combinations of these series are available in the market and literature, one of which is the Al-Ti-B alloy. AlTiB has been widely used as an additive material in the industry due to the strong grain-refining effect provided by its TiB_2 and Al_3Ti phases [4].

The AlTiB alloy system is observed to be primarily used as an additive rather than its direct use in the literature and industry. Yu et al. [5] demonstrated that the addition of Al–Ti–B promotes heterogeneous nucleation, resulting in significant grain refinement. Pengting et al. [6] demonstrated that the Al–3Ti–1B–0.2C master alloy provides higher refinement efficiency compared to the conventional Al–5Ti–1B system. Man et al. [7] reported that the addition of Al–Ti–B increases microstructural homogeneity in cast alloys, leading to increases in hardness and tensile strength. Arendarchuck et al. [8] emphasized that the addition of Al–Ti-B alloys positively affects wear and corrosion behavior. The grain-refining efficacy of Al–Ti–B alloys is primarily attributed to TiB_2 particles acting as potent heterogeneous nucleation substrates for α-Al grains during solidification. Fan et al. [9] confirmed, through high-resolution electron microscopy, the existence of a Ti-rich Al_3Ti two-dimensional compound (2DC) monolayer on the (0001) TiB_2 surface; this interfacial layer substantially enhances the nucleation potency of TiB_2 and is stabilised by sufficiently high solute Ti concentrations in the melt. Studies in the literature generally demonstrate the function of AlTiB as an additive alloy; no studies have been conducted on the behavior of the master alloy as a standalone material.

In contrast, information on the properties of the AlTiB master alloy in ingot form is quite limited. However, AlTiB ingots have long been produced in industry and are used solely for additive purposes [10]. The presence of hard and chemically stable TiB_2 and Al_3Ti phases suggests that AlTiB may exhibit independent mechanical and electrochemical properties beyond its additive role [11]. These properties suggest that AlTiB could be considered not only as an additive alloy but also as a potential material for direct use. However, one of the primary factors limiting the widespread use of AlTiB is its higher production costs compared to conventional aluminium alloys. However, detailed elucidation of the material's properties and its development through appropriate processes could contribute to overcoming this limitation. Basak et al. [12] illustrated that the in-situ formation of Al_3Ti and the ex-situ dispersion of TiB_2 particles within an aluminium matrix significantly enhance hardness and tensile strength, thereby affirming the reinforcing capabilities of these phases when incorporated into a bulk aluminium matrix. Kocaman et al. [13] synthesized functionally graded Al/(TiB_2+Al_3Ti) composites from an AlTiB master alloy and demonstrated that the distribution and proportion of these phases influence corrosion behavior in NaCl solution, underscoring the intricate role of phase morphology in the electrochemical response.

Studies on the corrosion behaviour of heat-treated AlTiB master alloys are quite limited in the literature, with existing research focusing primarily on grain refinement mechanisms during the casting process. This study aims to investigate the corrosion responses of AlTiB alloys heat-treated at different temperatures, providing new insights into the potential of AlTiB to be used not only as an additive but also as a standalone material under service conditions. In this respect, the study aims to contribute to the existing knowledge in the literature and lay the groundwork for future research and industrial applications.

2. Materials and Methods

A 10 mm diameter cylindirical rod of commercially available AlTi5B1 alloy was cut using a precision saw at a low cutting rate to avoid structural deformation. Four different samples were prepared in total, and heat treatment processes were applied on these samples at different temperatures. One sample was kept in the as-received condition named as bare sample. The remaining samples were separately incubated in an oven at 200 °C, 300 °C, and 400 °C for 30 minutes to assess the effect of temperature on the formation and properties of the passive surface film under the same exposure time [14]. After subjected heat treatment processes, specimens were taken out from the furnace and cooled in air.

With the characterization of Fourier transform infrared spectroscopy (FTIR) technique optical characterization for the AlTiB specimens were completed. Obtained FTIR spectroscopy results were provided via using Perkin Elmer spectrophotometer. Spectra were carried out for the AlTiB alloy specimens, recorded from 400 to 4000 cm−1.

Hardness test also carried out to catch a viewpoint observe the change of the mechanical properties of the heat-treated samples. LHV-1 (Bulut Makina, Turkiye) was used to achieve the micro-vicker test with a diamond pyramid indenter. To provide precise and accurate hardness results every tested surface of specimens were tested five times and averaged under the 0.5 kg load.

Corrosion studies were achieved with performing of the linear sweep polarization technique at room temperature. An Ametek Versastat 3 potentiostat and CView data analysis software were used to observe corrsion current density (Icorr) and corrosion potential (Ecorr). %3.5 NaCl aqueous solution was prepared with commercially available analytical grade NaCl (Tekkim, Turkiye) and deionized water. Titanium coated platin mesh was employed as counter electrode in the electrolyte environment. A silver/silver chloride (Ag/AgCl) electrode with saturated KCl solution was used as the reference electrode, while the AlTiB alloy specimens (heat-treated and non-heat-treated) served as the working electrodes. The surface area of the working electrodes submerged in the electrolyte was determined to be 78.54 mm^2, equivalent to the circular cross-section of a specimen with a diameter of 10 mm. Polarization scans commenced just below the open-circuit potential (OCP) and progressed positively at a scan rate of 2 $mV \cdot s^{-1}$. Two linear sweep voltammetry scans were performed for each specimen to ensure repeatability of the each sample.

3. Results and Discussions

The FTIR spectra of the AlTiB specimens are represented in Figure 1. This figure was employed to comprehend changes on the surface of the AlTiB alloy and exposed the heat treatment under the different temperatures as 200 °C, 300 °C and 400 °C in the muffle furnace. This figure displays the FTIR spectra, with the x-axis denoting the wavenumber (cm-1) and the y-axis representing absorption strength, labeled as transmission (%). The greater absorption peaks correspond to the vibrational modes of functional groups present on the alloy surface.

Any conspicuous peak was noticed in the spectrum of AlTiB without heat treatment. In this way, the chemical activity depending on heat treatment on samples were grasped by indicating higher absorption from measured area of the heat-treated samples. Presence of hydroxyl groups (-OH) through heat treatment was inferred from broad bands illustrated in the range around 3400 cm^{-1}, which intensified with increasing heat treatment temperature [15]. This broad band is associated with the O–H stretching vibrations of surface hydroxyl groups and physically adsorbed water formed on oxidized metal surfaces, and its intensity, although low, increases with temperature, indicating an increase in the degree of hydration and hydroxylation on the surface. The weak features observed in the mid-infrared region, around 1600–1700 cm^{-1}, can be attributed to the H–O–H bending mode of molecularly adsorbed water, which is consistent with the formation of a hydrated oxide layer on the alloy surface. Metal oxide peaks were noticed in between 400 cm^{-1} to 600 cm-1, which are assigned as the metal oxide lattice vibrations in

the literature [16,17]. It is suggested that these peaks, which occur in this range and intensify with increasing heat treatment temperature, could be AlO peaks.

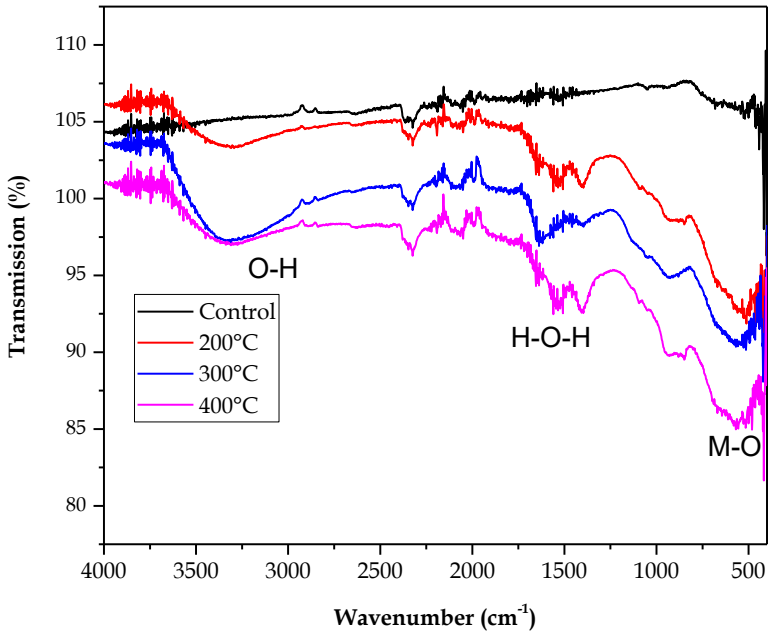


Figure 1 FTIR spectra of bare and heat-treated AlTiB alloy specimens showing characteristic peaks at ~3400 cm^{-1} (O–H stretching), ~1650 cm^{-1} (H–O–H bending), and ~400–600 cm^{-1} (metal–oxygen vibrations).

Figure 2 is given to comprehensively discuss of the corrosion behaviours for the non annealed and heat treated samples in 3.5% NaCl environment. Corrosion behavior was evaluated based on both corrosion potential and corrosion current density, where Ecorr indicates surface nobility and Icorr represents the corrosion rate. From the figure, corrosion resistance curves indicate that the corrosion potential becomes more positive for the samples heat-treated at 200 °C and 300 °C due to the influence of temperature. However, for the specimen heat-treated at 400 °C, the polarization curve shifts toward more negative potentials, suggesting increased electrochemical activity. Nevertheless, this parameter alone is not sufficient to evaluate corrosion resistance, and a more comprehensive assessment requires consideration of the corrosion current density (Icorr) [18] (Sünbül & İcin, 2024). In addition, the variation in current density observed at this temperature suggests that the electrochemical activity and corrosion rate of the alloy are strongly affected by the surface film properties formed during heat treatment. Furthermore, it was observed that changing the current density of the curve at this temperature can significantly affect the corrosion rate. To gain an understanding of the temperature-dependent electrochemical behavior, it is proposed that the Ecorr (corrosion potential, indicating surface nobility) and Icorr (corrosion current density, indicating corrosion rate) values be extracted from the curves presented in Figure 2, assessed quantitatively, and reported in Table 1. The incorporation of quantitative data facilitates a more visible comparison of how heat treatment of the alloy alters surface corrosion kinetics, allowing for an objective assessment of the surface transition from a passive to an active state [19].

Table 1 indicates that the corrosion potential (Ecorr) values were more positive t 200 °C (–0.5938 V) and 300 °C (–0.5694 V) than the untreated sample (–0.6793 V). This alteration indicates that passivation may be improved by the stability of surface oxides during mild thermal exposure. A notable negative shift of –0.8023 V was observed in the sample subjected to treatment at 400 °C, signifying the disruption of the protective coating and the reestablishment of a more active corrosion state. The corrosion current density (Icorr) exhibited a similar pattern, rising from 6.64×10^{-7} A/cm^2 in the untreated alloy to 4.91×10^{-6} A/cm^2 at 200 °C and 2.27×10^{-6} A/cm^2 at 300 °C, before quickly declining to 2.21×10^{-7} A/cm^2 at 400 °C. The non-monotonic alteration was construed as evidence that oxide production and surface activation were

facilitated by the first heat treatment, whereas further exposure at 400 °C correlated with the formation of a more stable and protective Al_2O_3 layer. Corrosion resistance of the Al–5Ti–B alloy showed the non-linear behavior, with the better performance observed at 400 °C. Although the corrosion potential (Ecorr) shifts to more negative values at 400 °C, the significantly lower Icorr indicates improved corrosion resistance, which could be attributed to the formation of a stable passive oxide layer. This enhancement can be attributed to the formation of a stable and compact oxide layer that effectively suppressed anodic dissolution. Such behavior can be explained by passivation, where the oxide film reduces corrosion kinetics despite the more negative corrosion potential [20].

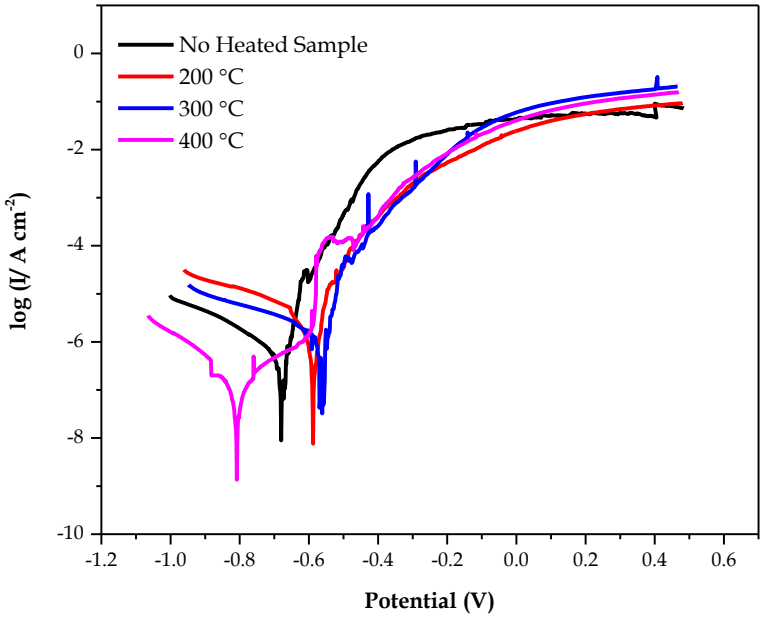


Figure 2 Potentiodynamic polarization curves of ALTiB alloy at different heat treatment temperatures

Table 1 Corrosion potential (Ecorr) and corrosion current density (Icorr) of AlTiB alloy specimens.

Sample	Ecorr (V vs Ag/AgCl)	Icorr (A/cm²)
Control	–0.6793 ± 0.012	$6.64 \times 10^{-7} \pm 3.0 \times 10^{-8}$
200 °C	–0.5938 ± 0.015	$4.91 \times 10^{-6} \pm 2.5 \times 10^{-7}$
300 °C	–0.5694 ± 0.011	$2.27 \times 10^{-6} \pm 1.2 \times 10^{-7}$
400 °C	–0.8023 ± 0.017	$2.21 \times 10^{-7} \pm 1.5 \times 10^{-8}$

Based on the Tafel curves in Figure 2 and quantitative corrosion values in Table 1 corrosion rate could be calculated through using Eq(1).

$$CR = (K \times Icorr \times EW) / \rho \quad (1)$$

Where K is the corrosion rate constant (3.27×10^{-3} mm·g·μA^{-1}·cm^{-1}·year^{-1}) used to convert the corrosion current density (ICorr) into a uniform corrosion rate in milimeters per year depending on ASTM G102 [21]. The density of the alloy which is defined as was utilized a value of 2.70 g·cm^{-3} for aluminum for being a base metal of the specimens alloy. The equivalent weight (EW) indicates the theoretical weight reduction of the alloy associated with one equivalent of oxidation, computed from the chemical composition of the AlTi5B1 alloy (Al = 95%, Ti ≈ 5%, B ≈ 1%), yielding a value of roughly 9.0 g·equiv^{-1}. The calculation was performed by considering the contribution of each element based on its atomic weight and valence (Al^{3+}, Ti^{4+}, B^{3+}) in accordance with ASTM G102.

Using the formula, illustrated corrosion rate results are given in Figure 3. The change depend on the heat treatment temperature was found as remarkable because of the non-linear behavior of the response. A

dramatical increase was detected after heat treatment process at 200 °C from 7.24 µm year^{-1} to 53.47 µm year^{-1}. This heat-treated specimen was also observed as have a highest corrosion rate per year. It was observed that with increasing heat treatment temperature, the quality of the passive film increased, especially at 400 °C, reaching a corrosion rate of 2.4 micrometer year-1, 2.5 times slower than the normal passive film.

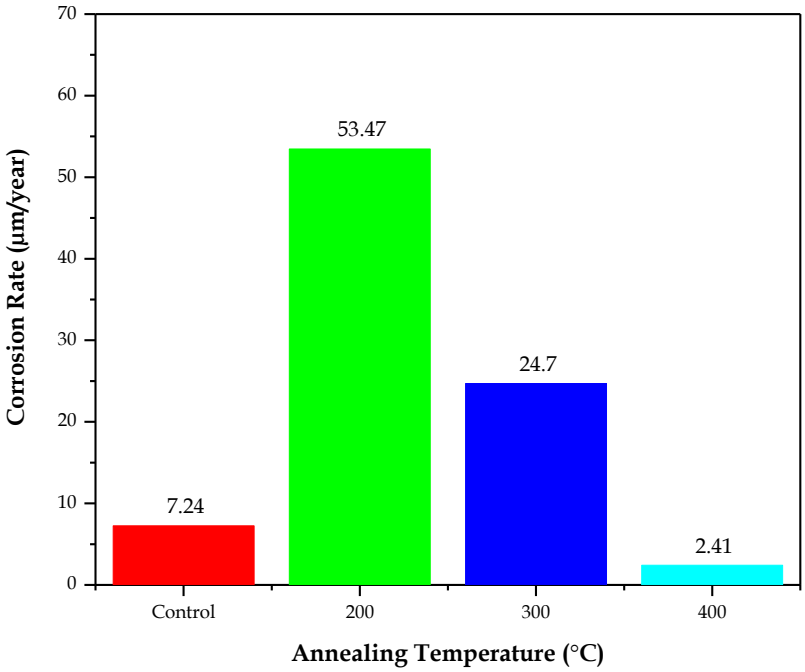


Figure 1 Corrosion rate change with respect to annealing temperature

Micro hardness results of bare and annealed AlTiB alloy specimens are shown in Figure 4. A similar trend was observed in the microhardness graph as in the corrosion rate variation shown in Figure 3. Although a slight increase in hardness was observed in the specimen heat-treated at 200 °C compared to the control sample, a significant decrease in hardness values was observed with increasing temperature. The decrease in hardness with increasing temperature indicated that the material experienced thermal softening during the annealing process.

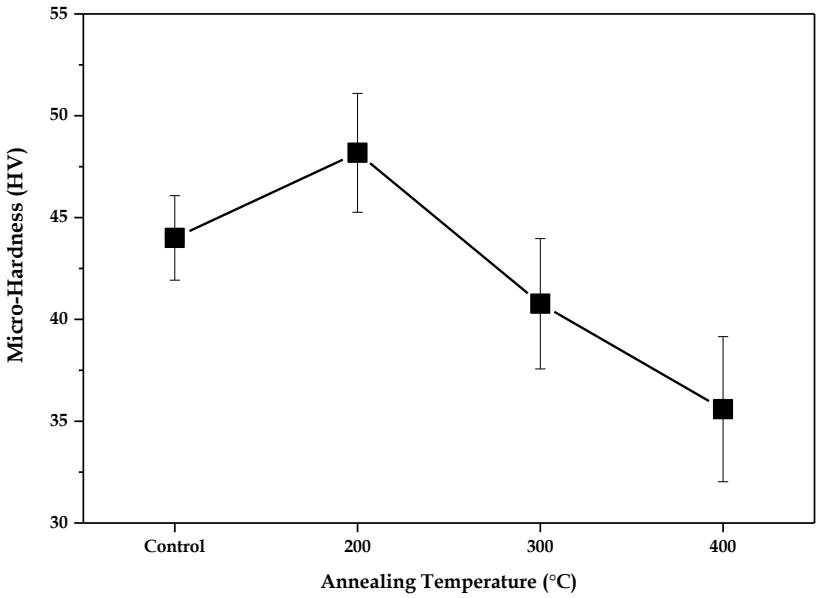


Figure 2 Microhardness change depend of annealing temperature

4. Conclusion

In this study, the effects of heat treatment on the corrosion behaviour and hardness of the Al-Ti-B master alloy were studied. Different temperature levels as 200ºC, 300 ºC and 400 ºC were carried out to complete annealing progress in muffle furnace for 30 minutes. The alterations on the surface of the heat-treated alloys were analyzed using FTIR spectra, revealing a rise in the intensity of hydroxyl and metal-oxide-related bands with elevated temperature, therefore suggesting surface oxidation and the formation of an oxide coating. The corrosion resistance and corrosion rate measurements were utilized to assess the electrochemical performance of both heat-treated and untreated samples. Even though corrosion resistance was improved from 200 °C to 300 °C, it did not exceed that of the untreated sample, whereas a significant improvement was achieved at 400 °C. This enhancement is ascribed to the development of a dense and stable oxide film that effectively limited anodic dissolution compared to the untreated and lower-temperature-treated samples. In contrast, the hardness behavior showed a different trend, where a slight increase was observed at 200 °C, while a noticeable decrease occurred at 300 °C and 400 °C, indicating thermal softening of the material. This study provides a promising perspective by demonstrating that well-known alloys such as Al–Ti–B can exhibit significantly improved and more balanced performance when subjected to appropriate heat treatment conditions, particularly in applications requiring enhanced corrosion resistance. The results indicate that Al–Ti–B has potential not only as a grain refiner but also as a standalone material for structural and functional applications.

Statement of Conflict of Interest

The author or authors of the article declare that they have no personal or financial conflict of interest with any institution, organization or person

References

[1] Ran Q, Shi H, Meng H, Zeng S-P, Wan W-B, Zhang W, et al. Aluminum-copper alloy anode materials for high-energy aqueous aluminum batteries. Nature Communications 2022;13:576. https://doi.org/10.1038/s41467-022-28238-3

[2] Kablov EN, Antipov VV, Oglodkova JS, Oglodkov MS Development and application prospects of aluminum–lithium alloys in aircraft and space technology. Metallurgist 2021;65:72–81. https://doi.org/10.1007/s11015-021-01134-9

[3] Langelandsvik G, Akselsen OM, Furu T, Roven HJ. Review of aluminum alloy development for wire arc additive manufacturing. Materials (Basel) 2021;14:5370. https://doi.org/10.3390/ma14185370

[4] Vicario I, Poulon-Quintin A, Lagos MA, Silvain JF. Effect of material and process atmosphere in the preparation of Al-Ti-B grain refiner by SHS. Metals (Basel) 2015;5:1387–96. https://doi.org/10.3390/met5031387

[5] Yu L, Liu X, Wang Z, Bian X. Grain refinement of A356 alloy by AlTiC/AlTiB master alloys. Journal of Materials Science 2005;40:3865–7. https://doi.org/10.1007/s10853-005-2893-8

[6] Li P, Liu S, Zhang L, Liu X. Grain refinement of A356 alloy by Al–Ti–B–C master alloy and its effect on mechanical properties. Materials&Design 2013;47:522–8. https://doi.org/10.1016/j.matdes.2012.12.033

[7] Zhu M, Yang G, Yao L, Cheng S, Zhou Y. Influence of Al-Ti-B addition on the microstructure and mechanical properties of A356 alloys. Rare Metals 2009,28:181–6. https://doi.org/10.1007/s12598-009-0036-0

[8] Fan Z, Wang Y, Zhang Y, Qin T, Zhou XR, Thompson GE, Pennycook T, & Hashimoto T. Grain refining mechanism in the Al/Al–Ti–B system. Acta Materialia 2012;84:292–304.

[9] Arendarchuck BE, Mayer AR, de Oliveira WR, Pukasiewicz AGM, Lourençato LA, Fals HDC, et al. Effect of Ti-B grain refiners on wear and corrosion of the A332 alloy with Sr modification. Applied Siciences 2022;13:430. https://doi.org/10.3390/app13010430

[10] Kosovich AA, Belyaev SV, Bogdanova TA, Partyko EG, Stepanenko NA, Tanachev LE, et al. Statistical analysis of parameters of the process analysis of grain refinement of the aluminum cast alloy by Al–Ti–B and Al–La–B master alloys. Metallurgist 2025;1–15. https://doi.org/10.1007/s11015-025-01902-x

[11] Basak S, Biswas P, Patra S, Roy H, & Mondal MK. Effect of TiB2 and Al3Ti on the microstructure, mechanical properties and fracture behaviour of near eutectic Al-12.6 Si alloy. International Journal of Minerals, Metallurgy and Materials 2021;28(7):1174–1185.

[12] Kocaman E, Aydın H, Yiğit K, Çalışkan F, & Savaş Ö. Corrosion behaviour of Al/(TiB2+-Al3Ti)-based functional grade metal matrix composite by sedimentation method. Transactions of the Indian Institute of Metals; 2024;77(8):2153–2161.

[13] McQuaig Jr MK, Toro A, Van Geertruyden W, & Misiolek WZ. The effect of high temperature heat treatment on the structure and properties of anodic aluminum oxide. Journal of Materials Science 2011;46(1):243–253.
[14] Li Q, Liu X, Wang J, Xue C, Wang S. Boosting the grain refinement of commercial Al alloys by compound addition of Sc. Journal of Materials Research and Technology 2024;28:1774–83. https://doi.org/10.1016/j.jmrt.2023.12.125
[15] Vijayadarshan P, Mohan T, Viswanath JV, Venugopal KJ, Rao NVS, Gupta A. Large scale synthesis of nickel oxide (NiO) by self propagated combustion reaction. Material Science Research India 2017;14:37–42. http://dx.doi.org/10.13005/msri/140106
[16] Hezam A, Namratha K, Drmosh QA, Yamani ZH, Byrappa K. Synthesis of heterostructured Bi2O3–CeO2–ZnO photocatalyst with enhanced sunlight photocatalytic activity. Ceramics International 2017;43:5292–301. https://doi.org/10.1016/j.ceramint.2017.01.059
[17] Sünbül SE, & İcin K. Evaluation of Tribological and Electrochemical Properties of Multiphase CoCuFeNiNb High Entropy Alloy. Ordu Üniversitesi Bilim ve Teknoloji Dergisi 2024;14(1):176–190.
[18] Yavuz A, Yilmaz NF, Kalkan MF. Enhancement in the Corrosion Resistance of Nickel Metal Via a Straightforward Thermal Oxidation Method. Journal of Bio-and Tribo-Corrosion 2023;9:22. https://doi.org/10.1007/s40735-022-00740-7
[19] Kim H, Bae S, Ji K, Kim SM, Yang JW, Lee CH, Lee KD, Kim S, Kang Y, & Lee HS. Passivation properties of tunnel oxide layer in passivated contact silicon solar cells. Applied Surface Science 2017;409:140–148.
[20] Hacıibrahimoğlu MY, Bedir M, Yavuz A. Structural and corrosion study of uncoated and Zn-Cu coated magnesium-based alloy. Metals (Basel) 2016;6:322. https://doi.org/10.3390/met6120322
[21] Li H, Wang B, Yang J, Xiao G, Tan S.The electrochemical corrosion behavior of Ti-5Al-5Mo-5V-1Cr-1Fe titanium alloy with different initial microstructures. Materials Today Communications 2024;39:108975. https://doi.org/10.1016/j.mtcomm.2024.108975